International Research Journal of Engineering and Technology (IRJET) e-ISSN: 2395-0056
Volume: 10 Issue: 02 | Feb 2023 www.irjet.net p-ISSN: 2395-0072

Investigating the Effect of Prestressing CFRP Laminate and Mechanical Anchorage to Strengthen Steel Beams Under Flexural Loading

Mohamed A. Gharib [1], Ali El Awadi [2]

[1] *alfanar Engineering Services, mo.g.abdul.76@gmail.com*
[2] *Teaching and Research Assistant, Zagazig University, Zagazig, Egypt, cengag2@gmail.com*

Abstract - *The use of composite materials, such as Carbon Fiber Reinforced Polymer (CFRP), as a strengthening and retrofitting method for steel beams, has gained widespread attention in recent years. This study aims to improve the understanding of the behavior of steel beams reinforced with CFRP laminates with mechanical anchorage. The previous analytical studies did not include the effect of mechanical anchorage. This study examines the behavior of steel I-beams strengthened with prestressed carbon fiber reinforced polymer (CFRP) laminate and fixed with mechanical anchorage under flexural loading. An experimental program, a closed-form analytical model, and a finite element analysis are presented in this investigation. Ten steel beams were experimentally investigated with and without mechanical anchorage and at various prestressing levels. An analytical and a finite element model considering the mechanical anchorage were developed to predict the stresses in the CFRP-Steel beam adhesive layer at the contact area. The models were validated with experimental results. The mechanical anchorage successfully increased the bond strength and changed the failure mode from premature debonding to CFRP rupture. The study highlights the importance of considering mechanical anchorage in analytical models for bonded CFRP laminates to ensure the preservation of prestressing force.*

Key Words: CFRP, Mechanical Anchorage, Prestressing, Cohesive Zone Methos, Crack Propagation.

1. INTRODUCTION

The use of CFRP laminate in retrofitting substandard steel beams is not popular as its use for retrofitting concrete structures [1 & 5]. The strengthening process includes the adhesion of a CFRP layer to the steel beam lower flange [2 & 3]. This configuration has a major problem which is the debonding failure of between the steel beam and the CFRP strip. It was found from previous studies that prestressing the CFRP layer may improve the performance utilize the full capacity of the strengthened hybrid beam.

Previous investigations found that prestressing the CFRP laminates is beneficial to the strengthening process [4]. Several techniques are suggested to apply the pretension force to the CFRP laminate in such a configuration. Mechanical anchorage is required for the effectiveness of these techniques. The proposed mechanical anchorage is applied at both ends of the laminate. This can result in an enhanced ductile behaviour and increase the prestressing force that can be applied. Using mechanical anchorage improves the serviceability and strength of the composite sections [2 & 6]. Previous studies that employed the finite element method to investigate the behaviour of this strengthening technique used the smeared crack concept to analyse the interfacial stress resulting from the contact zone between the steel beam and the CFRP laminates [7]. On the other hand, the discrete damage method reflects the final damaged condition more accurately. It models the crack propagation through a displacement–discontinuity using an interface element that separates two sides of the crack modelled using solid elements such as the cohesive zone method (CZM). This method presupposes that the stress between two surfaces of two materials does not dissipate immediately when damage is initiated at their interface. The cohesive material behaviour controls the interface between the separating surfaces of the steel beam and the laminate. The CZM act as a spring between the element connecting the modelled surfaces. However, the stiffness of the element is part of the structural stiffness, so the element deformation will occur during the loading of the laminate. Analytical models in previous studies were introduced to calculate the shear and normal stress in the contact zone between the steel surface and the CFRP layer attached to it [8, 9 &10]. However, these studies did not consider the significant effect of mechanical anchorage if employed.

This study utilized an experimental program to evaluate and analyze the behavior of steel beams reinforced with prestressed CFRP using mechanical anchorage under flexural loading at two points. A total of ten steel beams reinforced with various configurations of prestressed CFRP laminates were subjected to static flexural loading until failure occurred. The specimens were simulated using the CZM approach and finite element method. The accuracy of the FE model was validated by comparing it with the results obtained from the experimental program. The FE model was then utilized to evaluate the impact of increased prestressing. Furthermore, an analytical investigation was introduced to predict the interfacial shear and normal stresses on the adhesive layer of the examined beams. The analytical model's findings were compared against both the FEM and experimental program results.

2. THE EXPERIMENTAL PROGRAM

The experimental program considered several key factors, including the prestressing levels, yield strength of the steel beam, and mechanical anchorage implemented at both ends of the CFRP laminate. The jacking system setup shown in Figures (1) and (2) is used to apply the load to the strengthened beams.

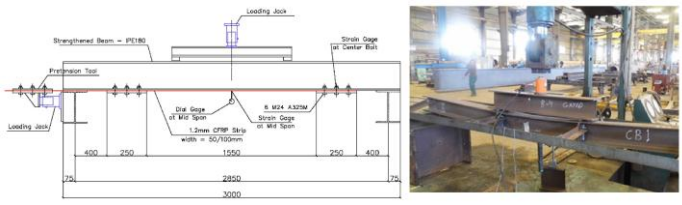

Fig -1: Test Setup

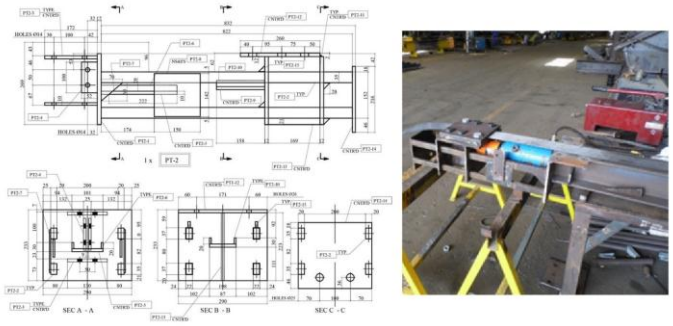

Fig -2: Test sample preparation and applying the pre-stressing force / prestressing tool detail

2.1 Description of the Beams

The experimental program's test specimen details are presented in Table (1). The first specimen has a section size of IPE160, while the other nine beams have a cross-section of W 6x20, with a steel beam length of 2.9 m. Specimen CB2 was reinforced with bonded CFRP and was not prestressed. The CFRP laminate thickness used for all specimens was 1.2 mm.

Table -1: Test Specimen Details

Specimen	CFRP laminate	Anchorage	Pretension Force (KN)
TB	50	Yes	NA
CB1	No	No	NA
CB1A	No	No	NA
CB2	100	No	NA
B1-25-NA	100	No	25
B2-45-NA	100	No	45
B3-25-AN	100	Yes	25
B4-45-AN	100	Yes	45
B5-25-AN	50	Yes	25

The CFRP laminate used to reinforce the specimens is 100 mm wide, with the exception of TB and B5-25-AN, which have a 50 mm wide CFRP strip. The thickness of the CFRP laminates for all specimens is 1.2 mm. Specimen B6-45-AN-NAD features a 100 mm pre-stressed CFRP laminate and mechanical end anchorage, but no adhesive layer was applied between the steel beam's lower flange and the CFRP laminate. Figure (3) illustrates the beam's cross-section and the CFRP layer.

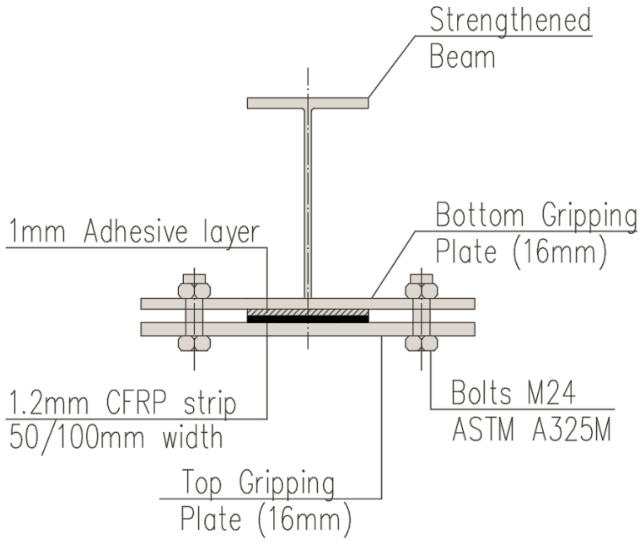

Fig -3: Cross section of the steel beam, adhesive, CFRP strip and the grip plates

2.2 Material Properties

The mechanical properties of the steel beam and the CFRP strips were determined through standard testing and from the manufacturer's datasheet. The average yield strength of the steel beam material is 390 MPa, and its ultimate tensile strength was measured to be 560 MPa.

The CFRP strips used in this investigation consist of pitch-based carbon fibers and epoxy resin, with thicknesses of 1.2 mm and widths of 50 mm or 100 mm. The fiber volume fraction of the strips is 68%. The CFRP laminate has an average ultimate strength of 3,100 MPa and an average measured elasticity modulus of 165 GPa [27].

A two-component epoxy adhesive was utilized to bond the CFRP laminate to the steel beam's surface. The adhesive's mechanical properties, as provided by the manufacturer's datasheet [28], are listed in Table (2).

Table -2: Properties of the epoxy material

Mechanical properties	Tensile strength	Compressive strength	Shear strength	Bond strength	Tensile modulus
Value (MPa)	24.8	61	24.8	18	4,400

2.3 Test Set-up

Figure (1) depicts the experimental setup used in this study, which consists of simply supported beams subjected to two-point loads. The load was applied to the beam using a universal testing machine. To measure the deflection, a displacement transducer was installed at mid-span. Additionally, strain gauges were mounted on the CFRP laminate and at the mid-span of the beam flanges to measure strain.

2.4 Experimental results

2.4.1 Failure Modes

In this study, applying prestressing to the CFRP laminate resulted in a proportional decrease in deflection and delayed premature debonding failure. The control beams CB-1 and CB-1A failed in a typical flexural manner. On the other hand, beam CB-2, strengthened with non-prestressed CFRP laminate, experienced a 1.2% increase in the failure load due to laminate debonding.

CFRP-prestressed beams B1-25-NA and B2-45-NA failed due to debonding of the CFRP laminate from the steel bottom flange immediately after releasing the grip anchor at both ends of the beam. However, CFRP-prestressed beams B3-25-AN and B5-25-AN with end anchorage and Fy = 390 MPa failed in a typical flexural manner, with the CFRP laminate experiencing a sudden rupture failure and a significant increase in the failure load compared to the non-strengthened control beam CB-1. These beams developed a full plastic hinge at failure without encountering premature debonding. The same failure mode was observed for beam B4-45-AN, but with a lower achieved strength enhancement of 3.3% in yield load.

The behavior of beam B6-45-AN-NAD, which had end anchorage but no adhesive, was similar to that of beams with end anchorage and adhesive in terms of flexural behavior, but the increase in failure load was less than for specimens strengthened using the adhesive layer, at 7% compared to the original non-strengthened beam CB-1. The CFRP laminate in this beam ruptured at a load of 186 kN, earlier than in the corresponding specimen with end anchorage and adhesive layer.

Table 3 provides a summary of the results obtained from the experimental investigation.

Fig -4: Typical CFRP rupture in tested beams

Table-3a: Results of the experimental investigation - Yield Load

Beam No.	CFRP Jacking Strain (με)	Yield Load P_y (kN)	P_y / P_{yCB}%
TB	3050	108.1	-
CB1	–	172.7	-
CB1A	–	161.0	-
CB2	–	174.8	-
B1-25-NA	3092	N/A	-
B2-45-NA	4021	N/A	-
B3-25-AN	3140	193.0	12%
B4-45-AN	3984	166.3	3%
B5-25-AN	3103	195.2	13%
B6-45-AN-NAD	4011	184.3	6.5%

Table-3b: Results of the experimental investigation – Debonding Load

Beam No.	CFRP debonding load		CFRP Failure
	P_{de} (kN)	Associated Strain (με)	
TB	No debonding	No debonding	No Failure
CB1	N/A	N/A	N/A
CB1A	N/A	N/A	N/A
CB2	193.2	5290	Debonding

B1-25-NA	64.8	15.16	Debonding
B2-45-NA	76.33	16.48	Debonding
B3-25-AN	204.5	3953	Rupture
B4-45-AN	178.9	5725	Rupture

Table-3c: Results of the experimental investigation-Rupture Load

Beam No.	CFRP rupture load		CFRP Failure
	P_{fru} (kN)	Associated Strain (□□)	
B3-25-AN	199.7	4435	Rupture
B4-45-AN	190.5	9601	Rupture
B5-25-AN	202.3	12101	Rupture
B6-45-AN-NAD	186.0	857	Rupture

2.4.2 Load-displacement relationship

The specimen TB failed due to lateral torsional buckling, but no debonding or CFRP rupture was observed during the test. The predicted yield load of the specimen was Py=93.3 kN. However, based on experimental results, the measured yield load was 108.16 kN at a corresponding deflection of 22.44 mm. This indicates a 16% increase in the yield load capacity of the strengthened section when compared to the predicted yield load.

The load deflection response of specimen B5-25-AN was compared to that of the control beam CB1. During the test, there was no debonding or CFRP rupture observed in B5-25-AN. The yield load of CB1 was 172.7 kN at a corresponding deflection of 20.46 mm, whereas the yield load of B5-25-AN was 195.2 kN at a corresponding deflection of 26.28 mm, indicating a 13% increase in the yield load capacity of the combined strengthened section. The final failure load of B5-25-AN was 200.7 kN at a corresponding deflection of 93.45 mm, while the final failure load of CB1 was 187 kN at a corresponding deflection of 82.63 mm.

Specimen CB2 attained its yield capacity without any observed premature failure. The yield load of specimen CB2 was measured to be 174.8 kN at a corresponding deflection of 19.5 mm, indicating that the CFRP strengthening, with neither prestressing nor mechanical anchorage, only increased the yield strength of the combined section by 1.2%. However, the specimen experienced a debonding failure and a sudden drop in the applied load after further loading. The debonding load for specimen CB2 was measured to be 193.2 kN at a corresponding deflection of 29.33 mm. After debonding, the specimen was un-strengthened and behaved similarly to control beam CB1 until final failure.

The load deflection response of specimen B3-25-AN was compared to that of the control beams CB1 and CB2. The yield load for specimen B3-25-AN was measured to be 194.66 kN at a corresponding deflection of 21.07 mm, indicating a 13% increase in the yield load capacity of the combined strengthened section compared to control beam CB1. During the plastic stage, the specimen experienced a load drop, combined with a sudden deflection at mid-span caused by CFRP rupture at a load of 199.7 kN and a corresponding deflection of 37.05 mm. The specimen exhibited a second and final rupture at a load of 197.8 kN at a corresponding deflection of 57.53 mm before the section became un-strengthened and had the same behavior as both control beams until final failure.

The load deflection response for specimen B4-45-AN was compared to that of control beam CB1A. Both specimens reached their yield capacity without any premature failure observed. The measured yield load for specimen CB1A was 161 kN at a corresponding deflection of 22 mm, while the measured yield load for specimen B4-45-AN was 166.3 kN at a corresponding deflection of 23.34 mm. This indicates only a 3.3% increase in the yield load capacity. Both specimens, B6-45-AN-NAD and CB1, exhibited similar load deflection responses. The specimens failed in a typical flexural manner, with no premature failure observed. The measured yield load for the specimen was attained with no significant difference compared to the control beam.

Specimen B6-45-AN-NAD showed only a 7% increase in yield load capacity compared to the control beam CB1, with a measured yield load of 184.3 kN at a corresponding deflection of 24.71 mm. Which shows how is the effect of the lack of the adhesive layer on the response and the overall strength. However, after further loading, the specimen experienced a rupture failure with a sudden drop in the applied load. The measured rupture load for this specimen is 201.33 kN at a corresponding deflection of 39.67 mm. The specimen also exhibited a second and final rupture at a load of 202.33 kN at a corresponding deflection of 55.14 mm before the section became un-strengthened and behaved similarly to the control beam until final failure.

Figure (5) shows the effect of adding CFRP strengthening and the advantage of prestressing the CFRP laminate which enhanced the overall performance of the beam.

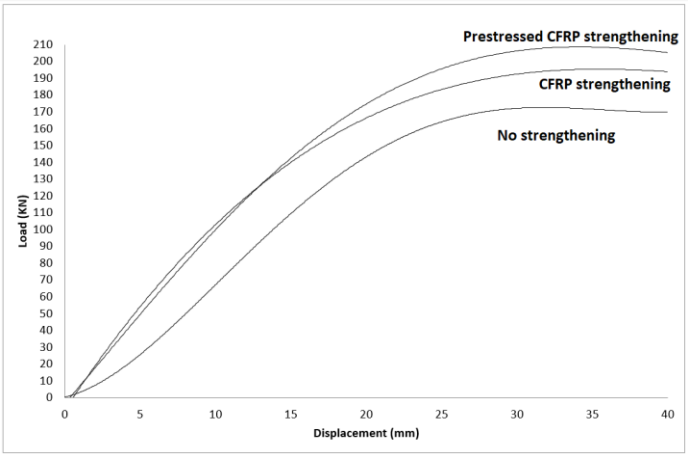

Fig-5: Load–displacement relationship for un-strengthened beam vs CFRP strengthened beam with and without prestressing

3 FINITE ELEMENT ANALYSIS

3.1 Finite element model

The finite element program ANSYS® (version 13) was used in this investigation [17]. A three-dimension element (3D FE) model was developed to simulate the geometric and nonlinear material behavior of the investigated beams. Four-node shell element, (Shell 281), was used to model the steel beam. Eight-node brick element (Solid 185) was used to model the adhesive layer and the CFRP strip [11]. The area between the CFRP laminate and the steel beam was simulated using a 3-D 8-node linear interface element (Inter 205). This element, when used with the (Solid185) element, simulated the interface between two surfaces and the subsequent separation process, where the separation was represented by a gradual displacement between nodes representing the two bonded surfaces.

3.2 Boundary conditions

Beams are symmetric about their longitudinal axis, and therefore only half of the beams were modeled. The beams were modeled with a roller support at one end and a hinged support at the other end. Two stiffening plates were welded to the steel beam's flange at the point of loading and at the supports to prevent stress concentration. The load was applied incrementally as a static load, following the automatic load control scheme. The modified standard/static general method was used for the analysis. Figure (6) depicts the simulated beam with applied forces and boundary conditions.

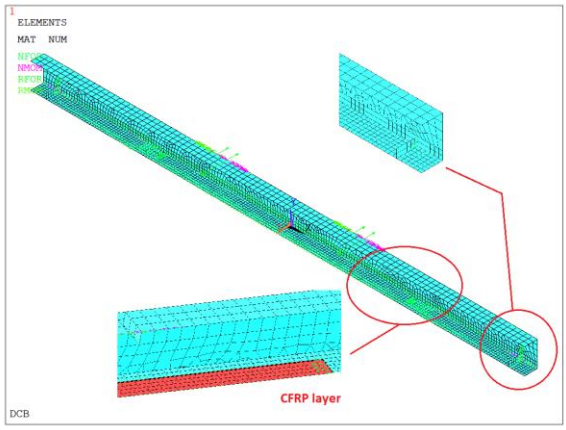

Fig -6: Simulated beam with boundary conditions

3.3 Materials modeling

In this study, the classical elastic-plastic material model with strain hardening was used to represent the steel I-beam, which has a bilinear stress-strain relationship for both compression and tension. The CFRP strip, on the other hand, has a linear stress-strain relationship until failure. When brittle materials undergo tensile fracture, microcracking, tortuous debonding, and other internal damage processes occur progressively and eventually lead to the formation of a geometrical discontinuity that separates the material. If this discontinuity occurs within the same material, it is called a crack, while if it occurs between two different materials, it is referred to as debonding or delamination. In this research, the cohesive zone modelling approach (CZM) is used to simulate debonding. To implement this approach, a CZ material was created and assigned to the contact elements in the interface zone, and its behavior is described in terms of a traction-separation equation instead of the traditional engineering stress-strain ($\sigma - \varepsilon$) equation. To ensure the zero thickness of the element, coincident opposite nodes of the cohesive element are defined. The CZ material was characterized by three constants: the material's maximum allowed stress, the energy release rate at normal separation, and the tangential displacement at maximum stress.

3.4 Prestressing Effect

There are many methods that can be used to simulate the prestressing effects on the CFRP laminates. In this investigation the constant prestressing effect in the laminate was applied in the longitudinal (x) direction to the specific material of the CFRP using the software package.

3.5 The Simulated Beams

The present study was conducted in two stages. Stage one focused on validating the present finite element analysis by analyzing numerically the steel beams that were previously tested in the experimental program. Five beams were

simulated at this stage to validate the finite element model. These included:

1. CB1: Control beam with no CFRP strengthening, having a steel yield strength of 390 MPa.
2. CB1A: Control beam with no CFRP strengthening, having a steel yield strength of 350 MPa.
3. CB2: Control beam with only one CFRP strengthening strip, 100mm wide, and a yield strength of 390 MPa. This beam was not subjected to any prestressing force. The CFRP strip was attached to the steel beam with a 1 mm layer of adhesive, without the use of mechanical anchorage.
4. B3: Beam strengthened with a 100 mm CFRP strip. The CFRP strip was subjected to 25 kN prestressing force. The yield strength of the steel beam was 390 MPa, and the CFRP laminate was attached to the steel beam using a 1 mm layer of adhesive material and two sets of mechanical anchorage, one at each end of the CFRP laminate.
5. B4: Beam similar in configuration to B3, but with a prestressing force of 45 kN and a yield strength of 350 MPa.

In the second stage of the study, the FEM model was extended to investigate the effect of increasing the prestressing level on the behavior of the beam. The validated FEM of the simulated beams from stage I was modified to evaluate the impact of increasing the prestressing force applied to the CFRP laminate. The beams tested at this stage were:

1. B3-15%: This beam has the same configuration as beam B3 introduced in stage I. However, the prestressing force applied to this beam was 15% of the ultimate tensile strength of the CFRP strip.
2. B3-40%: The prestressing force applied to this beam was 40% of the ultimate tensile strength of the CFRP strip.
3. B3-70%: The prestressing force applied to this beam was 70% of the ultimate tensile strength of the CFRP strip.
4. Figure (7) illustrates the load-displacement relationship for the simulated beam and the experimentally tested B4.

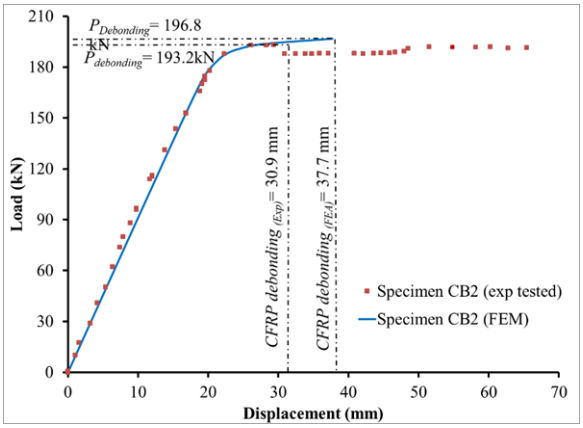

Fig -7: Load–displacement relationship for simulated beam and experimentally tested CB2

4 PROPOSED ANALYTICAL MODEL AND THEORETICAL APPROACH

The debonding failure mode is caused by interfacial stress concentration in the contact surface in the end zone. Closed-form solutions of such stresses are thus essential in developing any design guidelines for strengthening beams with bonded prestressing CFRP laminates.

Consider a steel beam with a typical I – section strengthened with a prestressed laminate bonded to the tension side.

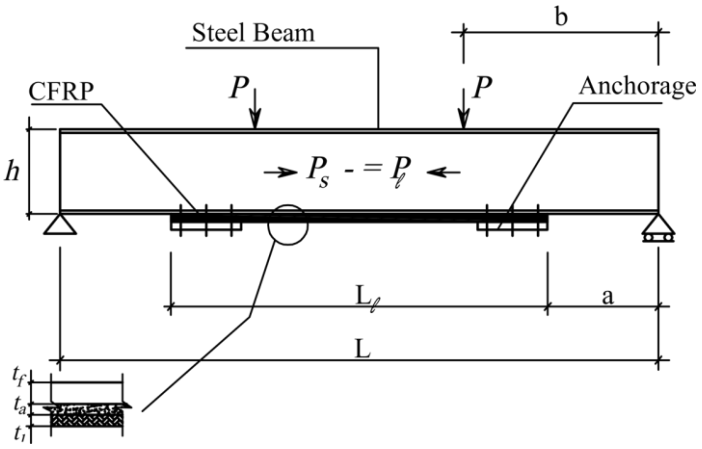

Fig -8: Schematic sketch of analyzed beam

For Simplification of the equations, the following assumptions were made:

- It is assumed that all materials exhibit linear elastic behavior.
- The stiffness of the steel beam is significantly greater than that of the CFRP laminate.
- The principle of the plane section remaining plane after deformation is upheld.

- Bending deformations of the adhesive layer can be disregarded.
- No slipping will occur at the interface area before failure.
- The thin adhesive layer thickness maintains constant stresses.

Figure (8) shows a schematic sketch of the beam strengthened with a bonded prestressed laminate where Pl is the residual prestressing force in the laminate.

The loss of prestressing force in the laminates is:

$$\Delta P_l = P_0 - P_l \quad (1)$$

However, in the case of using mechanical anchorage and applying adhesive layer, the loss of the prestressing P_l force can be neglected, and it can be assumed that $P_l = P_0$, hence the prestressing force in the steel beam P_s can be expressed as below:

$$P_S = -P_l \quad (2)$$

Analyzing a differential segment of a plated beam, where the interfacial shear and normal stresses are denoted by $\tau(x)$ and $\sigma(x)$, respectively [26], the interfacial shear stress can be calculated as per below equations:

1st Interval: for $0 \le x \le (b-a)$, at this interval, the general solution for the interfacial shear stress considering value of $V_s = P$, is

$$\tau_1(x) = B_1 \cosh(\lambda x) + B_2 \sinh(\lambda x) + m_1 P \quad (3)$$

2nd Interval: for $(b-a) \le x \le L_l$, at this interval, the general solution for the interfacial shear stress

$$\tau_2(x) = B_3 \cosh(\lambda x) + B_4 \sinh(\lambda x) \quad (4)$$

The solution for the above equation is:

$$\tau_1(x) = -B_2 e^{-\lambda x} + m_1 P - m_1 P \cosh(\lambda x) e^{-k} \quad (5)$$

and

$$\tau_2(x) = -B_3 e^{-\lambda x} \quad (6)$$

Where:

$$B_2 = -\frac{G_a}{\lambda t_a}\left[\frac{P_0}{E_s A_s} + \frac{Pah}{2E_s I_s}\right] \quad (7)$$

$$B_3 = \frac{G_a}{\lambda t_a}\left[\frac{P_0}{E_s A_s} + \frac{Pah}{2E_s I_s}\right] + m_1 P \sinh(k) \quad (8)$$

$$\lambda^2 = \frac{G_a}{t_a}\left[A_{11}^x + \frac{b_l}{E_s A_s} + \frac{h^2 b_l}{4E_s I_s}\right] \quad (9)$$

and

$$m_1 = \frac{G_a h}{2E_s I_s t_a \lambda^2} \quad (10)$$

$$k = \lambda(b-a) \quad (11)$$

And the adhesive normal stress can be expressed using below equations:

1st Interval: When $0 \le x \le (b-a)$,

$$\sigma(x) = e^{-\beta x}[C_1 \cos(\beta x) + C_2 \sin(\beta x)] - n_1\lambda(B_2 e^{-\lambda x} - m_1 P \sinh(\lambda x) e^{-k}) - n_2 \frac{P}{(x+a)} \quad (12)$$

2nd Interval: $(b-a) \le x \le L_l$,

$$\sigma(x) = e^{-\beta x}[C_1 \cos(\beta x) + C_2 \sin(\beta x)] - n_1\lambda B_3 e^{-\lambda x} - n_2 \frac{P}{(x+a)} \quad (13)$$

Where:

$$C_1 = \frac{P E_a}{2t_a\beta^3 E_s I_s}[1 - \beta a] + \frac{n_3}{2\beta^3}(m_1 P(1 - e^{-k} - B_2) + \frac{n_1}{2\beta^3}\left(-\lambda^4(B_2 + m_1 P e^{-k}) + \beta\lambda^3 B_2\right) \quad (14)$$

$$C_2 = \frac{(Pa)E_a}{2t_a\beta^2 E_s I_s} - \frac{n_1}{2\beta^2}\lambda^3 B_2 \quad (15)$$

5 RESULTS AND DISCUSSIONS

5.1 Analytical and numerical results

Tables (4) and (5) present the analytical and numerical results of the investigated beams. The results show that strengthening the beam with non-prestressed CFRP and without mechanical anchorage only increased the yield load Py of the beam by 1.2%. However, when prestressing and mechanical anchorage were used, the yield load increased from 1.2% to 11.7%.

Additionally, when the pretension load P_l was increased from 7% to 12%, the calculated adhesive shear stress at debonding load at peak τ_x=0 is reduced by 37%, and the calculated normal stress at debonding load at peak σ_x=0 was decreased by 30%. The FEM adhesive shear stress at debonding load at peak τ_x=0 is also decreased by 37%, and the FEM normal stress at debonding load at peak σ_x=0 was

decreased by 30% when the pretension load P_l is increased from 7% to 12%.

Table-4: Calculated interfacial Stress for the specimens tested in the experimental program

Sample	TB	B3-25	B4-45	B5-25
Prestressing Force P_0 (kN)	25	25	45	25
Premature Failure Load (kN)	108	199.7	178.9	202.3
Failure Mode	Torsional Buckling	CFRP Rupture	CFRP Rupture	CFRP Rupture
Calculated Peak Shear Stress (MPa)	34.4	31.5	28.7	32.8
Calculated Peak Normal Stress (MPa)	2.13	1.96	1.8	2.04

5.2 Calculated shear and normal stress on the adhesive layer at peak (laminates ends)

Figure (9) displays the shear and normal stress distribution at a loading value of 100 kN for the investigated beams TB, B3, B4, and B5 when strengthened without mechanical anchorage at both ends of laminates. In contrast, Figure (10) shows the same analysis for the beams after considering the mechanical anchorage in the analysis with the newly developed equations.

The analysis reveals that the mechanical anchorage neutralizes the effect of the mechanical properties of the adhesive layer and the prestressing level. The stress affecting the adhesive layer at both ends of the CFRP laminates is controlled only by the mechanical properties of the steel beam. These findings are consistent with the results obtained from the experimentally tested beam B6-45-AN-NAD.

Table-5: Experimental, Analytical and Numerical Results comparison

Beam No.	CB1	CB1A	CB2	B3	B4
Experimental Yield Load P_{Ey} (kN)	172.7	161	174.8	193	166.3
Numerical Yield Load P_{Fy} (kN)	172.8	158.4	174.4	193.6	164.8
Experimental CFRP debonding load P_{Ede} (kN)	N/A	N/A	193.2	204.5	178.9
Experimental CFRP rupture load P_{Eru} (kN)	N/A	N/A	No Rup.	199.7	190.5
Numerical CFRP debonding load P_{Fde} (kN)	N/A	N/A	193.6	212	187.2
Calculated Adhesive shear stress at debonding load at peak $\tau_{x=0}$	N/A	N/A	N/A	31.5	28.7
Calculated Adhesive Normal stress at debonding load at peak $\sigma_{x=0}$	N/A	N/A	N/A	1.96	1.8
FEM Adhesive shear stress at debonding load at peak $\tau_{x=0}$	N/A	N/A	0.13	7.94	3.61
FEM Adhesive Normal stress at debonding load at peak $\sigma_{x=0}$	N/A	N/A	0.94	2.38	1.93

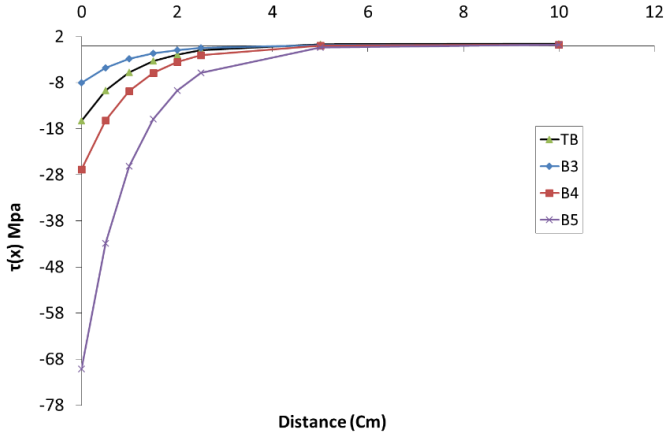

(a) Shear stress (MPa)

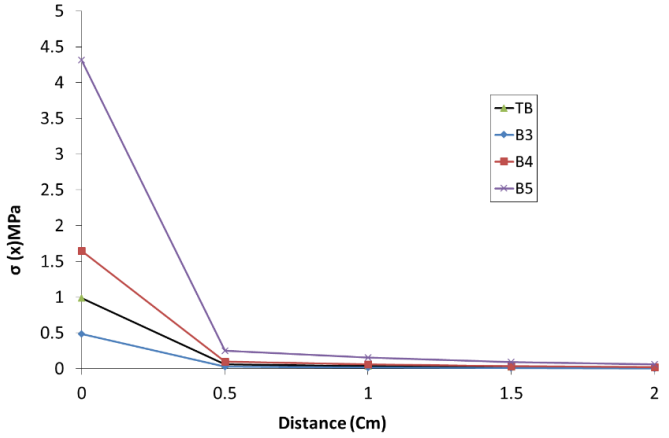

(b) Normal stress (MPa)

Fig. -9. Adhesive interfacial Stress at Fixed Load P=100 kN and variable Distance from Laminate End without mechanical anchorage.

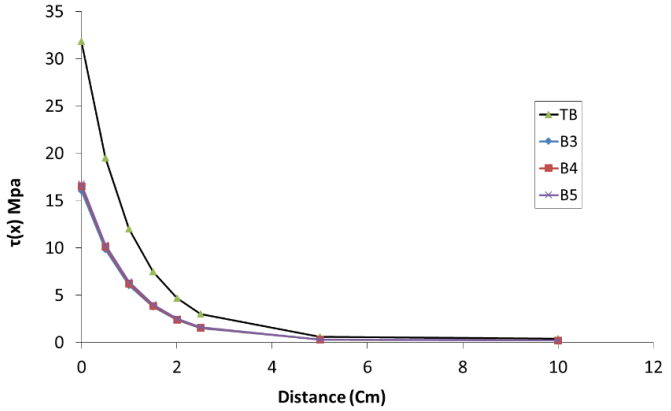

(a) Shear stress (MPa)

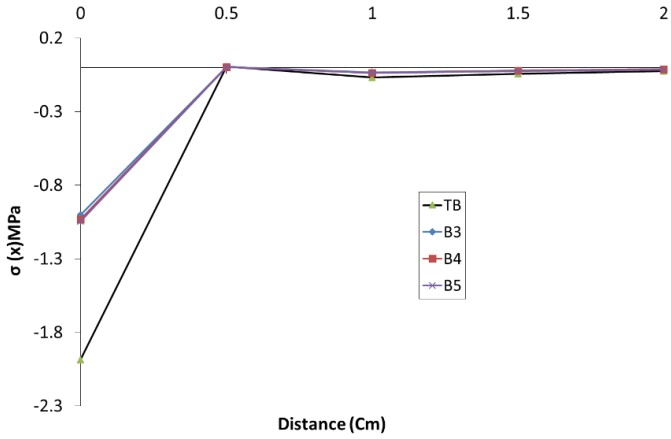

(b) Normal stress (MPa)

Fig. - 10. Adhesive interfacial Stress at Fixed Load P=100 kN and variable Distance from Laminate End with mechanical anchorage

5.3 Effect of pretension force level

To investigate the effect of the pretension force level on the peeling load, three beams were numerically studied: B3-15%, B3-40%, and B3-70%, with prestressing forces P_I of 55.8 kN (15% of the CFRP laminate ultimate tensile load), 140.8 kN (40% of ultimate tensile load), and 260.4 kN (70% of the ultimate tensile load of the CFRP laminate), respectively. These beams were compared with the original beam B3, which had a prestressing force P_I of 25 kN (almost 7% of laminate ultimate tensile load). A comparison between the present finite element analysis (FEA) and the experimental results is shown in Table 6, which presents the yield load and ultimate load for each specimen.

The results indicate that the applied loads versus mid-span deflections for the beams with different prestressing levels obtained from the FEA were almost similar. However, increasing the prestressing load P_I increases the yield load P_y and the overall composite section stiffness while decreasing the ultimate load capacity. Increasing the prestressing load up to 70% enhanced the section performance, but the failure mode changed from debonding to CFRP rupture. Therefore, it is recommended not to increase the prestressing level more than 40% of the laminate tensile capacity.

Table-6: B3 FEA Failure Loads

Beam No.	Yield Load P_y (kN)	Ultimate Failure Load P_U (kN)	Mode of Failure	P_U / $P_{U7\%}$
B3-7%	193.6	216	CFRP Debonding	1
B3-15%	196.8	219.2	CFRP Debonding	1.014
B3-40%	200	240	CFRP Debonding	1.11
B3-70%	N/A	135.2	CFRP Rupture	0.60

Previous studies have shown that increasing the prestressing force from 7% to 40% results in a significant decrease in normal stress along the length of the CFRP strip at a concentrated load of P=100 kN, with the stress peak point located at the mechanical anchorage at the ends of the laminate, which is consistent with the prediction of the developed analytical model [26]. Using the analytical model and assuming a prestressing force of 40%, the effect of increasing the adhesive layer thickness and the CFRP width was analyzed.

The results indicate that increasing the adhesive layer thickness has no significant effect on the shear stress at the peak point (x=a). However, increasing the adhesive layer thickness from 1mm to 2.5mm reduces the normal stress by 48%. Similarly, increasing the CFRP layer width from 5cm to 15cm reduces the calculated normal stresses by 3% at the peak load point when using a prestressing force of 45% at a 100kN point load.

Table - 7 provides detailed results from the analytical model.

Table-7 (a): Effect of increasing the adhesive layer thickness on the interfacial normal stress (at 100 kN load and 45% prestressing)

Adhesive thickness	Calculated normal stress at peak $\sigma_{x=a}$ (MPa)	Ratio
1mm	1.808	1
1.5mm	1.340	26%
2mm	1.084	40%
2.5mm	0.932	48%

Table-7 (b): Effect of increasing the CFRP laminate width on the interfacial normal stress (at 100 kN load and 45% prestressing).

CFRP laminate width	Calculated normal stress at peak $\sigma_{x=a}$ (MPa)	Ratio
5cm	1.834	0%
10cm	1.808	1%
12cm	1.798	2%
15cm	1.783	3%

3. CONCLUSIONS

In conclusion, the experimental and analytical studies carried out in this research provide valuable insights into the behavior of steel beams strengthened with CFRP laminates. It was found that the use of CFRP prestressing significantly increased the ultimate load capacity of the strengthened beam and delayed the premature debonding failure of the laminate. On the other hand, non-prestressed CFRP laminate mainly failed due to premature debonding, with only a slight increase in the failure load. The use of mechanical end anchorage was found to be essential in maintaining the CFRP laminate prestress after releasing the jacking force, while epoxy mortar alone was not sufficient for this purpose.

It was also observed that increasing the CFRP prestressing level up to 12-15% of the laminate tensile capacity, even without using a mechanical anchorage, provided significant enhancement in the ultimate load capacity of the beam and prevented premature debonding failure. The adhesive properties did not affect the ultimate load, but they may influence delaying the debonding of the laminates, which is highly dependent on the efficiency of the anchorage system and the level of prestressing. Thicker clamp plates were recommended to prevent prying action at prestressing grips.

An analytical model was presented to calculate the shear and normal stresses affecting the adhesive layer in the contact area between the CFRP laminate and the steel beam flange. The results of the analytical model were compared to those obtained from finite element analysis, and the accuracy of the calculations along the mid-span was found to be moderately satisfactory.

Finally, it was observed that increasing the prestressing force up to 40% enhanced the load capacity and bond strength of the steel-CFRP hybrid section, while higher prestressing levels led to premature rupture failure of the CFRP laminate, significantly reducing the section capacity. The optimum prestressing level was found to be 40% of the CFRP tensile capacity.

REFERENCES

[1] Young-Chan Youa, Ki-Sun Choia, and JunHee Kim, 2012. An experimental investigation on flexural behavior of RC beams strengthened with prestressed CFRP strips using a durable anchorage system, Composites Part B, ELSEVIER, 2012; 43:3026-3036.

[2] Miller, T. C., 2000. The rehabilitation of steel bridge girders using advanced composite materials." MSc. Thesis. University of Delaware, Newark, Delaware. USA.

[3] Miller, T.C., Chajes, M.J., Mertz, D.R., and Hastings, J., 2001. Strengthening of a steel bridge girder using CFRP plates. Journal of Bridge Engineering, ASCE, Vol. 6, No. 6, pp. 514-522.

[4] Young-Chan Y. A., Choi A. K., and Kim J. A., "An experimental investigation on flexural behavior of RC beams strengthened with prestressed CFRP strips using a durable anchor-age system". Composites. Part B, Engineering, ELSEVIER. 2012; 43: 3026-3036.

[5] Elawadi A., Orton S. L., Gopalaratnam V., Holt J., Lopez M. D. Accuracy Evaluation of Pre-stressed Concrete Girder Camber in Missouri Bridges. Journal of Bridge Engineering. Vol. 27, Issue 12 pp 04022119 (December 2022).

[6] Ghareeb, M.A, Khadr, M.A., Sayed-Ahmed, E.Y. CFRP Strengthening of Steel I-Beam against Local Web Buckling: A Numerical Analysis. Research and Applications in Structural Engineering, Mechanics & Computation: Proceedings of the Fifth International Conference on Structural Engineering, Mechanics & Computation, A. Zingoni (ed.), Taylor & Francis Group Ltd, Cape Town, South Africa, 2-4 Sept. 2013.

[7] M.H. Seleem, I.A. Sharaky, H.E.M. Sallam. Flexural behavior of steel beams strengthened by carbon fiber reinforced polymer plates – Three dimensional finite element simulation. Journal of Materials and Design, ELSEVIER. 2010; 31:1317-1324.

[8] Abdelrazik, A, Strengthening of steel I section Beam-Column using Prestressed CFRP Laminates, MSc. Thesis, Ain Shams University Faculty of Engineering, 2013, 154p.

[9] Youssef M. "Analytical prediction of the linear and nonlinear behavior of steel beams re-habilitated using FRP sheets". Journal of Engineering Structures, ELSEVIER. 2006; 28:903-911.

[10] Benachour A, Benyoucef S, Tounsi A, Adda bedia E. Inter-facial stress analysis of steel beams reinforced with bonded prestressed FRP plate. Journal of

Engineering Structures, ELSEVIER. 2008; 30:3305-3315.

[11] Zhao G, Li Alex. Numerical study of a bonded steel and concrete composite beam. Computer Structure 2008; 86 (19–20) :1830–8

[12] Sayed-Ahmed, E.Y. 2004. Strengthening of Thin-Walled Steel I-Section Beams Using CFRP Strips. Proceedings, 4th International Conference on Advanced Composite Materials in Bridges and Structures (ACMBS IV), Calgary, Alberta, Canada – CD Proceedings.

[13] D. Linghoff, M. Al-Emrani and R. Kliger, (2010) " Performance of steel beams strengthened with CFRP laminate – Part 1: laboratory tests" Composites Part B: Engineering, Vol. 41, No.7, p 509-515.

[14] D. Linghoff, M. Al-Emrani and R. Kliger, (2010) " Performance of steel beams strengthened with CFRP laminate – Part 2: FE analyses" Composites Part B: Engineering, Vol. 41, No.7, p 516-522.

[15] Al-Emrani M, Kliger R. Analysis of interfacial shear stresses in beams strengthened with bonded prestressed laminates. Journal of Composites Part B: Engineering, ELSEVIER. 2006; 37:265-272.

[16] Smith S., Teng J., (2001) "Interfacial stresses in plated beams". Journal of Engineering Structures, ELSEVIER. 2001; 23: 857-871.

[17] SAS, "ANSYS 10 Finite Element Analysis System", SAS IP, Inc 2004

[18] Sayed-Ahmed, E.Y. 2006. Numerical Investigation into Strengthening Steel I-Section Beams Using CFRP Strips. Proceedings, 2006 Structures Congress, ASCE, St. Louis, USA, 18-20 May 2006.

[19] Zhaoa, X., Zhang, L., (2007), "State-of-the-art review on FRP strengthened steel structures", Journal of Engineering Structures, ELSEVIER. 29: 1808-1823.

[20] Dawood, M., Rizkalla, S., and Sumner, E., (2007), "Fatigue and Overloading Behavior of Steel–Concrete Composite Flexural Members Strengthened with High Modulus CFRP Materials". Journal of Composites for Construction, Vol. 11, issue 6.

[21] Young-Chan Y. A., Choi A. K., and Kim J. A., "An experimental investigation on flexural behavior of RC beams strengthened with prestressed CFRP strips using a durable anchor-age system". Composites. Part B, Engineering, ELSEVIER. 2012; 43: 3026-3036.

[22] Youssef M. "Analytical prediction of the linear and nonlinear behaviour of steel beams rehabilitated using FRP sheets". Journal of Engineering Structures, ELSEVIER. 2006; 28:903-911.

[23] Sallam, H.E.M., Saba, A.M., Shaheen, H.H., and Abdel-Raouf, H. "Prevention of peeling failure in plated beams" Journal of Advanced Concrete Technology. 2004; 2(3):419-429.

[24] Lam, D. and Clark, K.A., 2003. "Strengthening of steel sections using carbon fiber rein-forced polymers laminate," Proceedings, Advances in Structures: Steel, Concrete, Composite and Aluminum ASSCCA'03, Sydney, Australia, pp. 1369-1374.

[25] El-Sisi A., Alsharari F., Salim H., Elawadi A., Hassanin A. "Efficient beam element model for analysis of composite beam with partial shear connectivity" Journal of Composite Structures. ELSEVIER. 2023; Vol. 303, 11626

[26] Gharib, M.A., Khedr., M.A., Sayed-Ahmed, E.Y. "Interfacial Stress of Steel Beams Strengthened with Prestressed CFRP Laminate And Mechanical Anchorage". Journal Of Al Azhar University Engineering Sector. Vol. 11, Issue 38, P:227-238.

[27] Sika Corporation, "Sika CarboDur® Carbon fiber laminate for structural strengthening," Identification no. 332, 2005.

[28] Sika Corporation, "Sikadur® 30 High-modulus, high-strength, structural epoxy paste adhesive for use with Sika CarboDur® reinforcement," Identification no. 332-15, 2008.